Buck Converter Common-Mode Emission with the Frequency Approach

Nassireddine BENHADDA[1], Abdelber BENDAOUD[1], Mohamed MILOUDI[1,2], Baghdadi BENAZZA[1,3], Soufyane BELHENINI[4]

[1]APELEC Laboratory, Djilali Liabes University, Sidi Bel-Abbès, Algeria

[2]Ahmed Zabana University, Relizane, Algeria

[3]Belhadj Bouchaib University, Aïn Temouchent, Algeria

[4] SS Laboratory, Belhadj Bouchaib University, Aïn Temouchent, Algeria

E-mail: benhadda_nasreddine@hotmail.com

***Abstract* –** Conducted electromagnetic emission for a DC/DC buck converter is predicted in this study using a frequency domain method. The noise source and noise path modeling taking into account parasitic elements of PCB traces and power electronic components while providing accurate conducted electromagnetic compatibility (EMC) noise levels. This approach will improve the conventional model by adding electromagnetic interference (EMI) generated during switching transients. In the common-mode (CM) model, the parasitic oscillation created during the turn-off of the diode and MOSFET is taken into consideration. The switching oscillation is simulated by an equivalent circuit. Finally, the complete CM model of the converter is implemented under the SPICE simulator in the frequency domain based on the Laplace Transform and confronted to experimental measurements. To test the robustness of the modeling method, simulation results are compared to measurements.

***Keywords* –** Buck Converter, Common-Mode, Direct Simulation Method, Laplace Domain, Parasitic Elements.

I. INTRODUCTION

Today, the recent development in power electronics has resulted in a considerable increase in the number of static converters. On the other hand, the evolution of the technology of semiconductor component in terms of volume reduction and high-frequency switching create more and more importantly electromagnetic interference (EMI). The study of electromagnetic compatibility has become a mandatory requirement for designers of power electronics circuits [1-5].

To predict the level of electromagnetic emissions emitted by a static converter, it must be modeled. The objective is to be able to evaluate the EMC impact of the converter at the conception phase [6-8]. Previous research has recommended two basic ways of the conducted EMI prediction, the time and frequency-domain approach. The time-domain approach uses circuit-simulation software and the noise spectrum is then obtained by a fast Fourier transform (FFT) [9, 10].

The time-domain simulation includes all phenomena related to conducted interference and allows the identification of the main sources and propagation paths. But the time of this type of simulation is very long, and there are also convergence problems encountered when the circuits become complex [11, 12]. The frequency-domain approach is preferable because it requires a shorter simulation time and has no convergence problem [9]. It’s based on the modelization of the emission sources by voltage or current equivalent generators and the propagation paths by localized impedances. In this paper, simplified models are developed for each mode to calculate conducted emission created by a static converter, the simulation results are obtained directly in spectral-domain and validated experimentally.

II. PRESENTATION OF THE CONVERTER

Figure 1 presents the scheme of the converter, it is supplied by V_{dc} = 42V through a Line Impedance Stabilized Network (LISN), the current load is I_{load} = 3 A. The operating frequency is 20 kHz. The principal components of the converter are the MOSFET IRFP

260 N, the diode BYT 08 P-400, and the decoupling capacitor. The parasitic elements of PCB trace and power electronic components are included, the common-mode parasitic capacitors are C_{L1_gnd}, C_{L2_gnd} and C_{mid_gnd}.

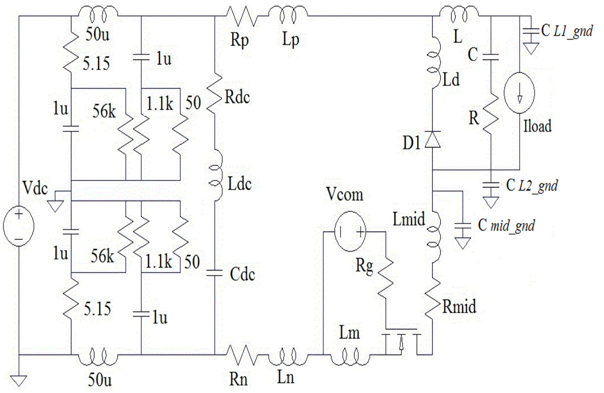

Fig. 1. Converter model [13].

III. FREQUENCY MODELING OF A CONVERTER

The common-mode noise can be predicted using three subcircuits together as shown in figure 2.

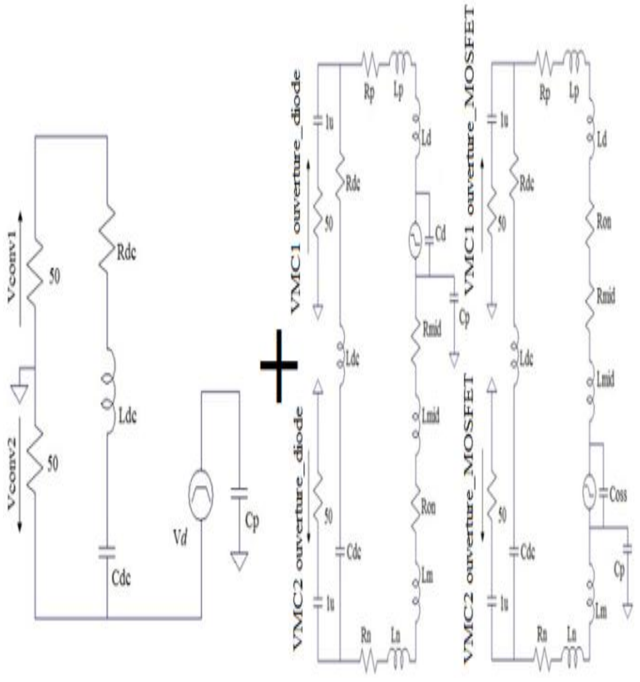

Fig. 2. Common-mode emission model.

The first is the low-frequency or conventional CM subcircuit [13-15]. It contains a voltage source V_{diode} a decoupling capacitor and the parasitic capacitance C_p.

Where: V_{diode} is a trapezoidal signal, its representation in Laplace domain is [16]:

$$V_{\mathrm{diode}} = \frac{2}{s^2} f_d V \left(\frac{1-e^{-st_r}}{t_r} - \frac{e^{-s\left(\frac{d}{f_d}+\frac{t_r}{2}-\frac{t_f}{2}\right)} - e^{-s\left(\frac{d}{f_d}+\frac{t_r}{2}+\frac{t_f}{2}\right)}}{t_f} \right) e^{-s\cdot\frac{d}{f_d}} \qquad (1)$$

Where: V is the voltage of DC bus; C_p is the CM propagation path [10, 17].

The two other high-frequency subcircuits are related to the switching oscillation phase. They contain a step current as an excitation source and a decoupling capacitor. The parasitics elements of PCB traces and power electronic components are taken into consideration [18].

IV. SIMPLIFICATION OF SIMULATION MODELS

In this section, a simple representation in LTspice simulator has been given, which will allow us to calculate rapidly the differential and common mode emission.

We can represent the switching phases (diode and MOSFET turn-off) in figure 3 by their functions of transfer $F_{Diode-off}$ and $F_{MOSFET-off}$ calculated by the equation (2) and (3) respectively.

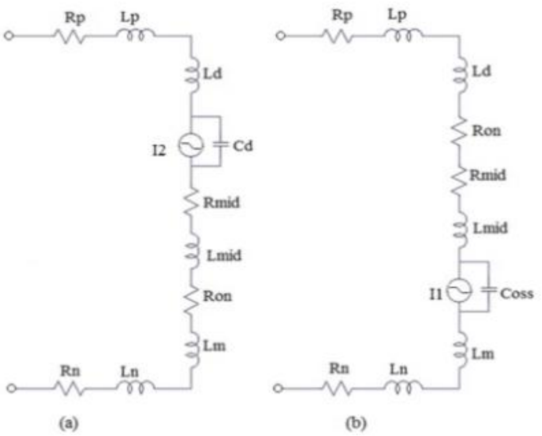

Fig. 3. Switching phases (a) turn-off of the diode, (b) turn-off of MOSFET.

We can represent the switching phases (diode and MOSFET turn-off) in figure 3 by their functions of transfer $F_{Diode-off}$ and $F_{MOSFET-off}$ calculated by:

$$F_{MOSFET-off} = \frac{1}{1+\frac{s}{Q_1\omega_1}+(\frac{s}{\omega_1})} \cdot I_1 \qquad (2)$$

$$F_{Diode-off} = \frac{1}{1+\frac{s}{Q_2\omega_2}+(\frac{s}{\omega_2})} \cdot I_2 \qquad (3)$$

Where: I_1 and I_2 represent the excitations, their frequency representations are given in (4) and (5) respectively [12, 13, 18].

$$I_1 = \frac{I}{t_r} \cdot \frac{1}{s^2} \cdot (1 - e^{-s\cdot t_r}) \qquad (4)$$

$$I_2 = \frac{I}{t_r} \cdot \frac{1}{s^2} \cdot (1 - e^{-s\cdot t_r}).e^{-s\cdot\frac{d}{f_d}} \qquad (5)$$

$$\omega_1 = \frac{1}{\sqrt{L_{eq1}C_{oss}}} \tag{6}$$

$$Q_1 = \frac{1}{R}\sqrt{\frac{L_{eq1}}{C_{oss}}} \tag{7}$$

$$\omega_2 = \frac{1}{\sqrt{L_{eq2}C_d}} \tag{8}$$

$$Q_1 = \frac{1}{R}\sqrt{\frac{L_{eq2}}{C_d}} \tag{9}$$

R is the sum of parasitic resistors of interconnections.

$L_{eq1} = L_{eq2}$ are the sum of parasitic inductances of interconnections.

Using the functions of transfer instead of the high-frequency subcircuits in figure 2, the novel simulation model of common-mode emission becomes as illustrated in figure 4.

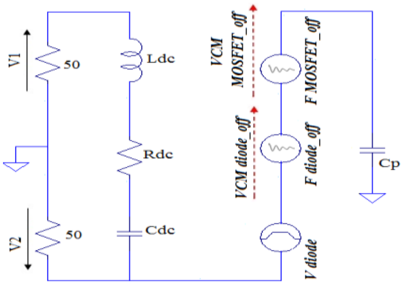

Fig. 4. Novel model of common-mode emission

The expression of common-mode voltage is written as follows:

$$V_{CM} = \frac{(V_1+V_2)}{2} \tag{10}$$

V. VALIDATION MEASUREMENT

Figure 5 shows the prototype of measurement used to validate the simulation models previously developed.

Fig. 5. Prototype of the conducted measurement

The experimental and simulation results of the common-mode emission are shown in figure 6.

A very good correspondence can be observed between the spectra obtained by the modeling method and the measurement across the entire frequency range (150 kHz - 30 MHz).

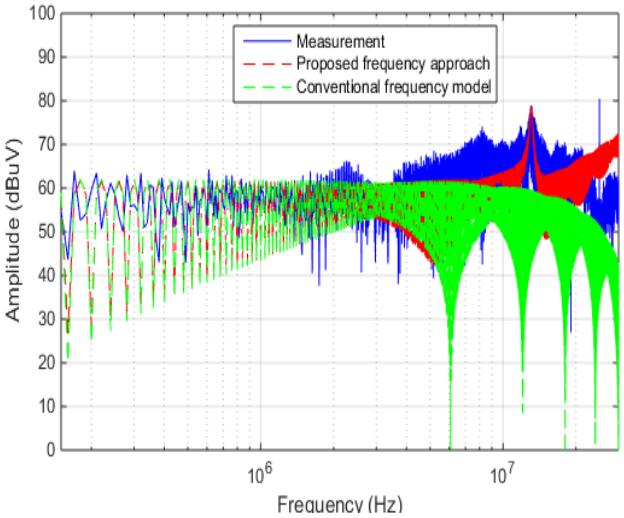

Fig. 6. Experimental and simulation results of the common-mode emission

VI. PARAMETRIC STUDY

The interconnections of printed circuit boards have been modeled using the method of moments, the simulator Q3D is based on this modeling method. For extracting the parasitic elements, the converter has been implanted in this simulator as shown in figure 7.

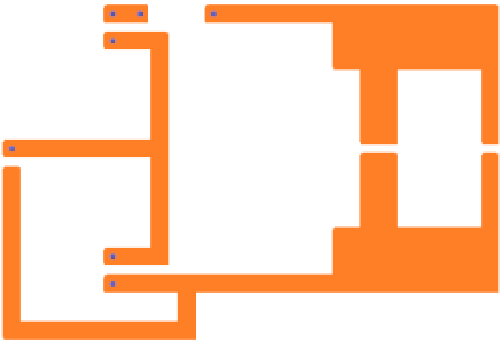

Fig. 7. Modeling of interconnections of printed circuit boards

To test the robustness of the modeling method developed previously, in this section we have made some changes to the parameters of the converter. A simulation study will be carried out and compared with measurements to see the influence of variation of each parameter on the common-mode conducted emission.

To observe the influence of parasitic inductances and resistances of trace on levels of conducted EMI, it has been chosen to realize the routing of the converter with more long-traces than the first.

The second routing used, is presented in figure 8.

Fig. 8. Second routing used.

The common-mode emission experimental and simulation results for both routings are shown in figure 9.

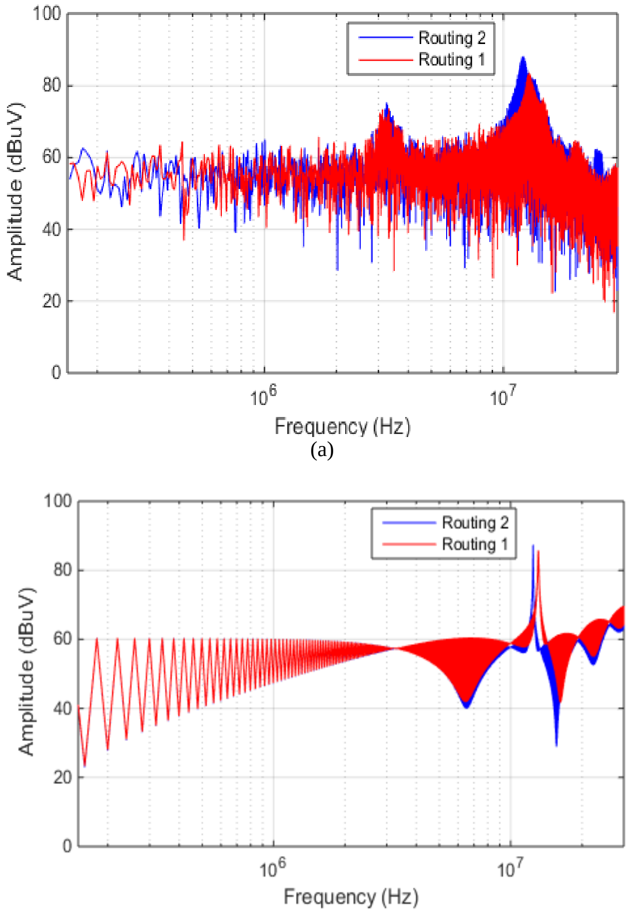

(a)

(b)

Fig. 9. Experimental (a) and simulation (b) results of common-mode emission for both routing

To observe the influence of operating frequency on the levels of conducted EMI, it has been realized measurement and simulation with a 20 kHz, 60 kHz, and 100 kHz.

The experimental and simulation results of the common-mode emission are shown in figure 10.

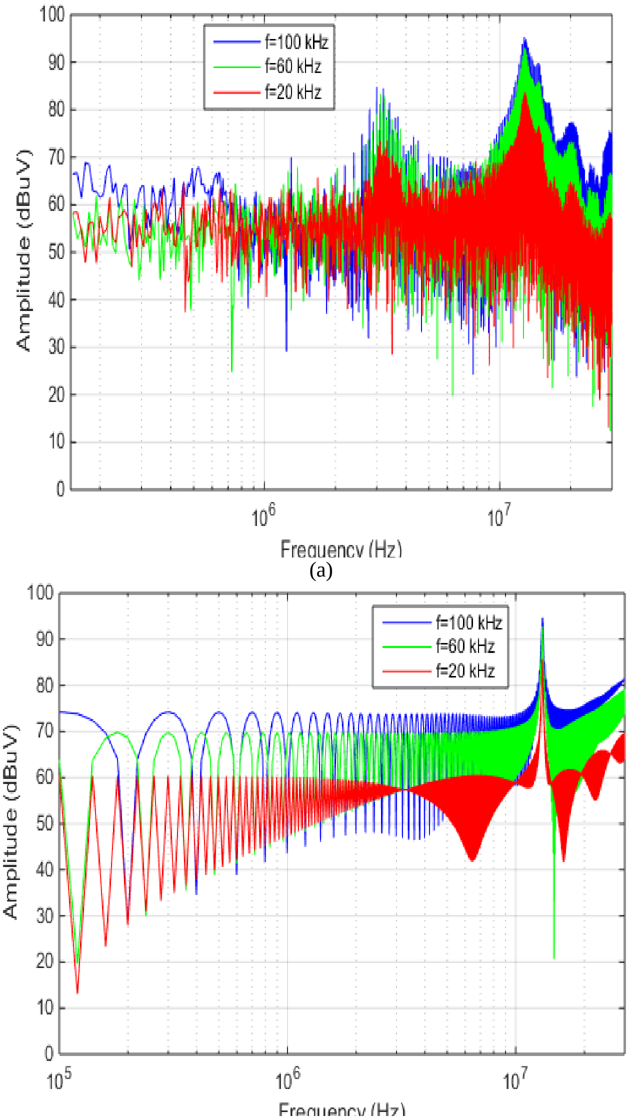

(a)

(b)

Fig. 10. Experimental (a) and simulation (b) results of common-mode emission at different switching frequencies.

In the previous section, experiments and simulations were performed with a 10 Ω gate resistor.

To show the influence of gate resistor on the levels of conducted EMI, experiments and simulations are made when the converter working with 20 Ω and 37 Ω resistances, and the results of the common-mode emission are presented in figure 11.

For each parameter, a very good correspondence can be observed between the spectra obtained by the modeling method and the measurement across the entire frequency range (150 kHz - 30 MHz).

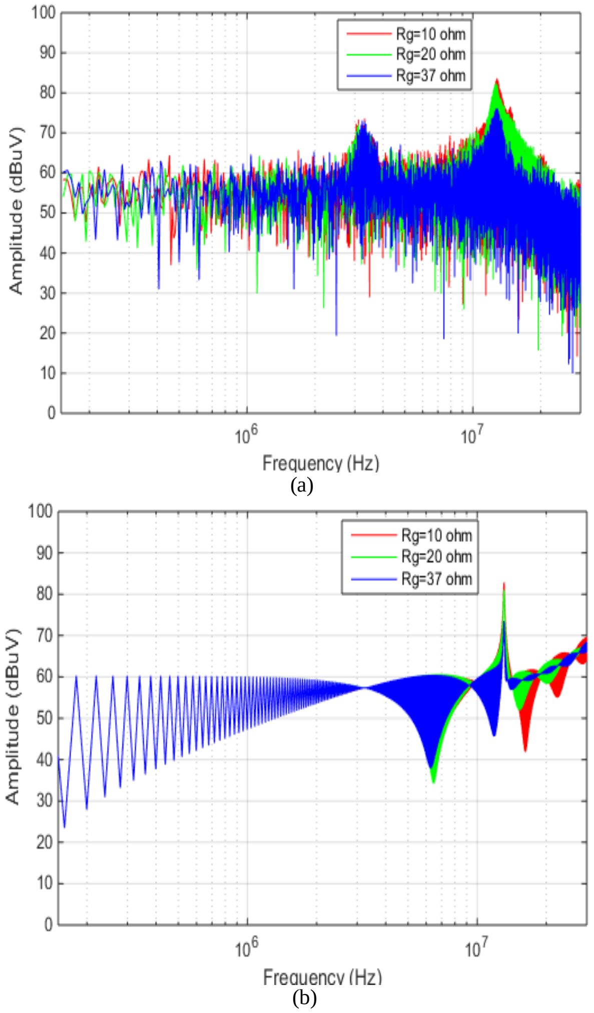

(a)

(b)

Fig. 11. Experimental (a) and simulation (b) results of the common-mode emission at different gate resistances

VII. CONCLUSION

This paper presents a frequency domain method for predicting electromagnetic interference (EMI) noise in DC/DC buck converter. Modeling of the noise source and noise path and taking into account parasitic elements of PCB traces and power electronic components allows accurate conducted EMC noise levels. In the adopted method the parasitic oscillation created during turn-off of diode and turn-off of MOSFET is adding to the conventional model. Based on the Laplace transform, the CM model is implemented under SPICE simulator in the frequency domain.

The comparison of simulation results to experimental results indicates the efficiency of the proposed method for the conducted EMI prediction in a DC/DC buck converter. The method can predict the impact of various parameters such as PCB routing, switching frequency, and gate resistance.

VIII. REFERENCES

[1] J-B. GROS, *Modelisation de l'immunite des circuits integres complexes aux perturbations electromagnetiques*, doctoral diss., University of bordeaux I, 2010.

[2] J. Ben Hadj Slama, *modélisation du rayonnement électromagnétique des circuits d'électronique de puissance. Application à un hacheur*, doctoral diss., university of Lyon, 1997.

[3] Mohamed Miloudi, Abdelber Bendaoud, Houcine Miloudi, Common and Differential Modes of Conducted Electromagnetic Interference in Switching Power Converters, *Revue Roum. Sci. Techn.* 62 (3), 2017, 246–251.

[4] C. Jettanasen, *modélisation par approche quadripolaire des courants de mode commun dans les associations convertisseurs-machines en aéronautique; optimisation du filtrage*, doctoral diss., university of Lyon, 2008.

[5] D. Labrousse, B. Revol, F. Costa, Switching Cell EMC Behavioral Modeling by Transfer Function, *Proc. of the 10th Int. Symposium on Electromagnetic Compatibility, Yourk, UK*, 2011.

[6] H. Bishnoi, A.C Baisden, P. Mattavelli, D. Boroyevich, Analysis of EMI Terminal Modeling of Switched Power Converters, *IEEE Transactions on Power Electronics, 27(9)*, 2012.

[7] L. Fakhfakh, A. Amous, New simplified model for predicting conducted EMI in DC/DC converters, *Springer-Verlag Berlin Heidelberg*, 2016.

[8] M. Moreau, *Modélisation haute fréquence des convertisseurs d'énergie. Application à l'étude des émissions conduites vers le réseau*, doctoral diss., university of Lille, 2009.

[9] V. Tarateeraseth, I.A. Maio, F.G. Canavero, Assessment of Equivalent Noise Source Approach for EMI Simulations of Boost Converter, *Proceedings, 20th Int. Zurich Symposium on EMC, Zurich*, 2009.

[10] L. Fakhfakh, A. Alahal, A. Amous, Fast Modeling of Conducted EMI Phenomena Using Improved Classical Models, *Asia-Pacific International Symposium on Electromagnetic Compatibility (APEMC)*, 2016.

[11] Houcine Miloudi, Mohamed Miloudi, Abdelber Bendaoud, A Method for Modeling a Common–Mode Impedance for the AC Motor, *Journal of Electrical Engineering and Computer Science 84 (5), 2017, 241–246.*

[12] X. Huang, *frequency domain conductive electromagnetic interference modeling and prediction with parasitics extraction for inverters*, doctoral diss., university of Blacksburg, Virginia, 2004.

[13] N. Benhadda, A. Bendaoud, N. Chikhi, A conducted EMI noise prediction in dc/dc converter using a frequency-domain approach, *Elektrotehniški Vestnik 85(3), 2018, 103-108.*

[14] B. Nassireddine, B. Abdelber, C. Nawel , D. Abdelkader , B. Soufyane, Conducted EMI prediction in dc/dc converter using frequency domain approach, *International conference*

on electrical sciences and technologies in Maghreb (CISTEM), Algeria, 2018.

[15] Z. Fedyczak, A. Kempski, R.Smoleński, Conducted high frequency disturbances observed in electrical power systems with switch mode converters, *Przegląd Elektrotechniczny,* R. 89 NR 6/2013.

[16] M. Nave, Prediction of conducted emissions in switched mode power supplies, IEEE Int. Symp. On EMC'86, pp 167-173,1986.

[17] P. Fernández-López, M. Bensetti, F. Duval, Low-impedance passive component modelling using S-parameter measurements, *16 ème édition du Colloque International sur la Compatibilité Électromagnétique (CEM),* 2012.

[18] Mohamed Miloudi, Houcine Miloudi, Abdelber Bendaoud, Mohammed Adnan Salhi, Ahmad N. Al–Omari, Experimental Characterization of the High–Frequency Isolating Power Transformer, *Journal of Electrical Engineering and Computer Science,* 86 (4), 2019, 211–218.